Article

Biochemical and EPR-spectroscopic Investigation into Heterologously Expressed Vinyl Chloride Reductive Dehalogenase (VcrA) from Dehalococcoides mccartyi strain VS

Anutthaman Parthasarathy, Troy A. Stich, Svenja T. Lohner, Ann Lesnefsky, R. David Britt, and Alfred M. Spormann

J. Am. Chem. Soc., **Just Accepted Manuscript** • DOI: 10.1021/ja511653d • Publication Date (Web): 16 Feb 2015

Biochemical and EPR-spectroscopic Investigation into Heterologously Expressed Vinyl Chloride Reductive Dehalogenase (VcrA) from *Dehalococcoides mccartyi* strain VS

Anutthaman Parthasarathy[1], Troy A. Stich[2], Svenja T. Lohner[1], Ann Lesnefsky[1], R. David Britt[2], and Alfred M. Spormann[1*]

[1]Departments of Chemical Engineering, and of Civil and Environmental Engineering, Stanford University, Stanford, CA,

[2]Department of Chemistry, University of California Davis, Davis, CA

[*]Corresponding author's address: James H. Clark Center, 318 Campus Drive, Stanford University, Stanford, CA

Phone: 650.723.3668, email: spormann@stanford.edu

ABSTRACT: Reductive dehalogenases play a critical role in the microbial detoxification of aquifers contaminated with chloroethenes and chlorethanes by catalysing the reductive elimination of a halogen. We report here the first heterologous production of vinyl chloride reductase VcrA from *Dehalococcoides mccartyi* strain VS. Heterologously expressed VcrA was reconstituted to its active form by addition of hydroxocobalamin/adenosylcobalamin, Fe^{3+}, and sulfide in the presence of mercaptoethanol. The kinetic properties of reconstituted VcrA catalyzing vinyl chloride reduction with Ti(III)-citrate as reductant and methyl viologen as mediator were similar to those obtained previously for VcrA as isolated from *D. mccartyi* strain VS. VcrA was also found to catalyze a novel reaction, the environmentally important dihaloelimination of 1,2-dichloroethane to ethene. Electron paramagnetic resonance (EPR) spectroscopic studies with reconstituted VcrA in the presence of mercaptoethanol revealed the presence of Cob(II)alamin. Addition of Ti(III)-citrate resulted in the appearance of a new signal characteristic of a reduced [4Fe−4S] cluster and the disappearance of the Cob(II)alamin signal.

UV-vis absorption spectroscopy of Ti(III)citrate-treated samples revealed the formation of two new absorption maxima characteristic of Cob(I)alamin. No evidence for the presence of a [3Fe-4S] cluster was found. We postulate that during the reaction cycle of VcrA, a reduced [4Fe-4S] cluster reduces Co(II) to Co(I) of the enzyme-bound cobalamin. Vinyl chloride reduction to ethene would be initiated when Cob(I)alamin transfers an electron to the substrate, generating a vinyl radical as a potential reaction intermediate.

INTRODUCTION

Chloroethenes, such as tetrachloroethene (PCE), trichloroethene (TCE), the dichloroethenes (DCE), vinyl chloride (VC), as well as the chloroethanes 1,1,2 trichloroethane (TCA), and 1,2 dichloroethane (DCA) are the most prevalent groundwater contaminants in developed countries including the United States [1-3]. Key for the microbial degradation of such chlorinated aliphatic hydrocarbons to harmless organic compounds are catabolic reductive dehalogenases (Rdh). Rdhs are highly oxygen-sensitive enzymes and catalyze the reductive elimination of a halide. The catalytically active subunit RdhA contains a corrinoid and two [4Fe-4S] clusters and is typically associated with the outer leaflet of the cytoplasmic membrane presumably via the small integral membrane protein RdhB. Rdhs are unique among the FeS cluster/corrinoid enzymes in that they catalyse a net reduction reaction directly by the cobalamin without the intervention of other organic cofactor radicals [4].

Current understanding of Rdh is limited to results from studies with only a few purified enzymes - PceA [5,6], CprA [7,8], TceA [9] and VcrA [10]. These studies indicated a relatively high degree of substrate specificity of each Rdh. More recently, dihaloeliminating reductive dehalogenases were identified, resulting in the formation of chloroethenes from chloroethanes [11,12]. Thus, the degradation of both classes of organohalogens intersect via a mosaic metabolic networks of diverse Rdhs [11]. Whether such dihaloeliminating activities are due to a single, mono- and dihaloeliminating Rdh or the concerted action of two specific Rdhs has not been revealed. However, dihaloelimination is of critical importance for successfully engineering bioremediation and avoiding accumulation of more toxic intermediates such as vinyl chloride.

Reductive dehalogenation is a catabolic process coupling energy conservation with a dehalogenation reaction. It is found primarily in the anaerobic *Dehalococcoides*-, *Sulfurospirillum*-, and *Dehalobacter*-type microorganisms. In *Dehalobacter restrictus*[13], *Desulfomonile tiedjei* [14] and *Sulfurospirillum multivorans* [15], reductive dehalogenation is one of many possible modes of energy conservation. In contrast, *Dehalococcoides sp.* are highly niche-specialized and can only conserve energy by reductive dehalogenation. *Dehalococcoides* Rdhs are unique and distinctive in that the electrons for chloroethene reduction are derived obligatorily from H_2. Hydrogen is presumably oxidized by a HupL hydrogenase, which appears to form a membrane-bound complex facing the outside of the cell with an Rdh (Fig S1) [16]. How the electrons are transferred to an Rdh, and how *Dehalococcoides* spp. conserve metabolic energy during this unique respiratory process, are unknown.

The development of a molecular understanding of *Dehalococcoides*-type Rdhs, in particular the study of the reaction mechanism has been hampered by the slow doubling time of the microorganisms, the low biomass yield, and the oxygen sensitivity of native Rdhs. Numerous unsuccessful attempts have been conducted by different research groups to heterologously produce active Rdhs. Only recently two reductive dehalogenases were heterologously expressed in the background of a dehalogenating strain: reductive dehalogenase (PceA) of *Desulfitobacterium hafniense* strainY51 was overexpressed in *Shimwellia blattae* [17] and the NpRdhA of *Nitratireductor pacificus* in *Bacillus megaterium* [18]. We report here the first successful heterologous overproduction in *E. coli* of a *Dehalococcoides*-type Rdh, its reconstitution to an active form, as well as its initial biochemical characterization.

EXPERIMENTAL SECTION

Plasmid construction: Standard protocols [19] were used for all genetic work. Promega kits were used for isolation and purification of DNA. Vector pLIC-HMK (a gift from Dr. James Berger, University of California, Berkeley) was used as the plasmid backbone. The *vcr*A gene (vinyl chloride reductase A) from *Dehalococcoides* VS (NCBI Gene ID: 8658217, NC_013552.1:complement(1187299-1188753)) devoid of the first 35 amino acids of the 5' region coding for the TAT-signal peptide was amplified from the genomic DNA of *Dehalococcoides mccartyi* strain VS using 5'- TAC TTC CAA TCC AAT GCA

GACATTGATGAACTTGTTTCAAGC – 3' as the upstream primer and 5' – T TAT CCA CTT CCA ATG TTA TTA AGTACCGGGATCAAAGCC – 3' as the downstream primer, and inserted into pLIC-HMK using ligation independent cloning or LIC [20] to create an IPTG inducible N-terminal, 6x-Histidine, Maltose Binding Protein (MBP), TEV protease cleavage site *vcr*A fusion gene [21,22]. Fermentas LIC qualified T4 DNA polymerase was used to perform the LIC reaction. The fidelity of the entire gene fusion was verified by DNA sequencing. This plasmid was denoted NNHM-VcrA for N-terminus, No TAT signal sequence, 6x-Histidine Tag, Maltose binding protein *vcr*A gene fusion. For simplicity we address the NNHM-VcrA protein in this manuscript as VcrA-MBP with the understanding that it is the fusion protein, as described here: refer to Fig S2.

Heterologous expression of VcrA-MBP in *E. coli*: pLIC-HMK NNHM-VcrA was transformed into chemically competent cells of *E. coli* BL21 DE3. 5 ml cultures of this strain were grown overnight at 37°C in non-inducing minimal medium (MDG medium [23]) supplemented with 2 g/L glucose and 100 μg/ml of kanamycin. The overnight cultures were then inoculated into LB medium supplemented with 0.2 % (w/v) of glucose and 100 μg/ml of Kanamycin up to an initial OD_{600} of 0.1. After the cultures had reached an OD_{600} of 0.5 at 37°C, expression of the plasmid was induced upon addition of 1 mM IPTG final concentration. Following 3 h of induction, the cells were harvested by centrifugation at 6000 × g at 4°C for 20 min on a Beckman Coulter Avanti J-20 XP centrifuge. The overproduction was verified by SDS PAGE. The bulk of the overproduced protein was found in the insoluble fraction (data not shown).

Purification of VcrA-MBP by affinity chromatography: 3 g of Ni-IDA or Ni-TED bonded to silica [24,25] for His-Tag affinity chromatography (Protino® Ni-IDA Resin & Protino ® Ni-TED Resin, Macherey Nagel) was added as slurry in distilled water to a 20 ml fritted column (diameter 2 cm) and allowed to pack by gravity to about 8 ml volume. Gentle suction was applied at the bottom of the column through a vacuum line to drain the aqueous phase. Dry columns were stored at room temperature until use.

All subsequent operations were carried out in a Coy anoxic chamber (95%N_2, 5%H_2). All buffers, filters, centrifuge tubes and columns were incubated at least overnight in the anoxic

chamber prior to use. Buffers and solutions were filtered through a sintered glass filter layered with Whatman GF/C 55 mm glass fibre filters and were subsequently subjected to 4 cycles of degassing and purging with nitrogen (99.99%). In the anoxic chamber 2 mM 2-mercaptoethanol final concentration was added to all solutions and buffers.

About 3 g wet weight of induced cells carrying pLIC-HMK NNHM-VcrA were re-suspended in ca. 30 ml of Buffer A (50 mM potassium phosphate pH 8.0 containing 0.5 M NaCl, 20% (v/v) glycerol and 1 mM PMSF as a protease inhibitor). After sonication in the anoxic chamber at 70% power for 15 min (30 s pulse followed by 30 s cooling) at 4°C, the suspension was centrifuged for 30 min at 4°C at 30,000 × g on a Beckman Coulter Avanti J-20 XP centrifuge. The supernatant was discarded and the pellet re-suspended in 15 ml of denaturing buffer (Buffer A + 8 M urea). Following another round of sonication at 70% power for 15 min (30 s pulse followed by 30 s cooling) at 4°C, the suspension was stirred on ice for 60 min to solubilize the pellet. Another centrifugation for 30 min at 4°C at 10,000 × g was performed to remove any remaining insoluble material.

The supernatant containing denatured VcrA-MBP was loaded onto the Ni-IDA column, which had been washed with 5 column volumes of Buffer A and equilibrated with 3 column volumes of denaturing buffer. VcrA-MBP elution was achieved with 3 column volumes of 250 mM imidazole in the denaturing buffer. The eluted fractions were collected and analysed separately. The samples were desalted with PD-10 columns (GE Healthcare) which had been previously washed with several volumes of anoxic buffer, to remove urea and imidazole, and eluted with Buffer A containing 0.2% CHAPS (3-[(3-cholamidopropyl)dimethylammonio]-1-propanesulfonate) as detergent. The eluted fractions were pooled and allowed to refold in the refolding buffer (50 mM Tris pH 8.0 containing 0.5 M NaCl, 20% (v/v) glycerol, 0.2% CHAPS and 1 mM PMSF (phenylmethylsulfonyl fluoride) as a protease inhibitor and 2 mM 2-mercaptoethanol) for 1 h at room temperature and then concentrated via Amicon Ultracel 50 K centrifugal filters (EMD Millipore) at 6000 × g on a Clay Adams Compact II centrifuge. The concentrated protein was mixed with a minimum volume of the refolding buffer and frozen at -80°C until further use. The purity of VcrA-MBP was verified by SDS-PAGE (Fig 1) and peptide mass fingerprinting of the corresponding SDS gel band.

Cofactor reconstitution: Anoxic solutions of 200 mM DTT, 100 mM $FeCl_3$ and 30 mM $Na_2S.9H_2O$ were prepared in degassed 100 mM Tris-HCl pH 7.4 purged with 99.99% N_2 prior to the cofactor reconstitution. In order to initiate the reconstitution of the iron-sulfur clusters of VcrA or VcrA-MBP, the protein was reduced by the addition of 5 mM DTT, and the solution was incubated at room temperature for 30 min to be completely reduced. The iron-sulfur clusters were subsequently reconstituted by adding $FeCl_3$ at 5 mol excess over protein and Na_2S at 10 mol excess over protein to the mixture, which was then incubated at room temperature for 90 min. Precipitated protein and iron sulfide particles were removed by centrifugation at 5,000 × g for 5 min. Finally, adenosyl- or hydroxocobalamin was added to a final concentration of 10 mg/ml, and the mixture was incubated at room temperature for 30 min. Unbound iron sulfide and cobalamin were removed by passage through PD-10 columns (GE Healthcare). The samples were filtered through 0.2 μm Thermo Scientific Nalgene® Syringe filters, eluted with the refolding buffer, concentrated to ca. 20 mg/ml and stored at -80°C until further use. The reconstitution of the enzyme could be performed with any one of the following B_{12} derivatives – adenosylcobalamin, hydroxocobalamin, dicyanocobinamide or aquahydroxocobinamide, although only the first two were used for trials involving activity assays.

TEV-protease digestion and purification of untagged VcrA: Samples of purified but unassembled VcrA-MBP apoprotein were digested anaerobically with manufacturer-recommended amounts of Pro-TEV (Promega) protease (which contains a HQ tag allowing for His-tagged affinity chromatography) in 50 mM Tris HCl pH 8.0 free of protease inhibitors for 3 h at 20°C to remove the MBP & His tags. The digest was passed over a Ni-IDA column which retained Pro-TEV protease via its HQ tag as well as the His-MBP tag of VcrA. The untagged VcrA (defined here and described as 'VcrA' as opposed to the parent 'VcrA-MBP') was collected from the flow through and confirmed pure by PAGE (Fig. S3); 3 mg of VcrA-MBP yielded 0.8 mg of untagged VcrA.

SDS-PAGE and protein determination: Samples for SDS-PAGE and protein quantification were prepared by using Zeba® Micro Spin desalting columns 7 MWCO (Thermo Scientific) following the manufacturer's protocol and eluted in distilled water. Further processing for SDS-PAGE was performed according to the NuPage® Novex system (Invitrogen). NuPage® Novex

1.0 mm BisTris 10-12% acrylamide precast gels (Invitrogen) were used for the PAGE analysis. The SeeBlue Plus2® Prestained Standard (Invitrogen) was used as a molecular weight marker. Protein concentrations were determined by the BCA assay using the Micro BCA® Protein Assay Kit (Thermo Scientific), using Bovine Serum Albumin as standard.

Metal analysis: For metal analysis, concentrated enzyme (either VcrA-MBP or VcrA) was desalted, eluted in distilled water, digested with 5 % HCl and filtered to remove the precipitated protein. Non-heme iron in the protein was quantified with Ferene (3-(2-pyridyl)-5,6-bis (5-sulfo-2-furyl)-1,2,4-triazine, disodium trihydrate) [26,27]. For the calibration curve, 2-20 μM standards were prepared freshly from a stock solution containing 0.2 mM $(NH_4)_2Fe(SO_4)_2.6H_2O$. The iron standards, the water reference and the protein-containing solutions were each filled with H_2O to a final volume of 100 μl. The solutions were mixed with 100 μL 1% HCl (v/v) and incubated at 80 ºC for 10 min. After cooling to room temperature 500 μl ammonium acetate 7.5% (w/v), 100 μl ascorbic acid 4% (w/v), 100 μl of SDS 2.5% (w/v) and 100 μl of Ferene 1.5% (w/v) were sequentially added into each sample with vortex mixing. The Eppendorf tubes containing the reaction mixtures were centrifuged at 13,000 × *g* for 10 min. The supernatant was used for measuring the UV-VIS absorbance at 593 nm. The iron content of the protein solution was calculated from the calibration curve of the absorbance.

Cobalt content was analysed by ICP-MS [28,29]. Solutions of 5 ml were prepared for the cobalt standards and samples of unknown concentration were prepared in clean unused plastic BD tubes in 5% HCl. The calibration curve was from 0.1 to 5000 parts per billion. The samples were analysed on a Thermo XSeries II ICP-MS, with a 60 s rinse of 3% nitric acid between samples and an uptake time of 60 s for each sample. 3 readings were collected and the average was reported. Internal standards of cobalt (2.5 ppm and 5 ppm) were used; scandium and yttrium were used for corrections.

GC methods: Chloro-ethenes and ethanes were quantified by gas chromatography using an Agilent Technologies 6890 Network GC System instrument equipped with a flame ionisation detector (FID) and an HP 624 Special Analysis column (capillary 30.0 m × 530 μm × 300 μm). The injector was maintained at 200°C, and the FID was operated at 280°C. Helium was used as

carrier gas (99.9% purity) at a pressure of 4.86 psi and a flow rate of 5.1 ml/min. The temperature program was 8.6 min at 100° C with no ramping.

VcrA activity assays: All enzyme activity experiments were performed in triplicates in anoxic, sealed crimped serum vials of 10 ml volume stoppered with butyl rubber stoppers, containing 6 ml of the aqueous phase and 4 ml of headspace. 0.1 ml headspace samples were injected into the GC for analyzes. Standards of ethene were prepared by diluting a commercial 1.01% standard (Supelco) into serum vials, assuming an ideal gas volume of 22.4 L per mole. For the chlorinated compounds, commercial standards of 2 mg/ml dissolved in methanol (Supelco) were diluted into the serum vials.

Henry's constants K_H^{cc} at 20°C from the US EPA website (http://www.epa.gov/athens/learn2model/part-two/onsite/esthenry.html) were used to calculate the partition of 1,1-DCE, VC and 1,2-DCA between gas and aqueous phases. For ethene, a K_H^{cc} of 7.6 was used [30]. Calibration curves obtained by correlating peak area and the number of moles were used for calculation of the number of moles observed in the enzymatic assays.

A typical assay mixture in an anoxic 10 ml serum vial contained 0.2-1 mg/ml of fully reconstituted VcrA, 1 mM Ti (III) citrate and 0.4 mM methyl viologen as electron donor and mediator, respectively, in 50 mM Tris-HCl pH 8.5. The reaction was started by injecting a defined volume of aqueous 1,1-DCE from a saturated aqueous solution of approximately 26 mM. For vinyl chloride a methanolic solution of 32 mM was used; for 1,2-DCA, an aqueous stock solution of 100 mM was used. The incubation time was generally 60 min; the 1,1-DCE concentrations and the incubation times were varied during different experiments. For cobalamin-only measurements, the same mixture was used; enzyme was omitted and 2 mg/ml cobalamin was added. After allowing the reaction to proceed for a specified time, the reaction was stopped by the addition of 0.1 ml of concentrated HCl.

Peptide Mass Fingerprinting (PMF): Mass mapping was performed at the PAN Center, Stanford University using a 4700 Proteomics Analyzer that features tandem (MS/MS) time-of-flight (TOF) optics to provide peptide structural information, in addition to high accuracy MS data. The data showed 25-60 ppm accuracy in mass mapping experiments without the need for

internal calibration. The laser repetition rate was 200 Hz. Sample preparation for PMF was carried out as follows: 45 mM dithiothreitol (Sigma) in 10 mM ammonium bicarbonate (pH 7.8) was added to polyacrylamide gel slices and then incubated for 30 min at 55°C. The solution was changed to 100 mM acrylamide (Bio-Rad) in 10 mM ammonium bicarbonate and incubated 1 h at room temperature. The ammonium bicarbonate solution was removed, and 0.5 ml of 10 mM ammonium bicarbonate and 50% acetonitrile was added to the gel and incubated for 30 min. The gel slice was then dried to completion. A small volume (2 to 10 µl) of 10 mM ammonium bicarbonate containing 4 to 20 pmol of trypsin (Promega) was added to the slice. The gel was then saturated with 10 mM ammonium bicarbonate buffer. Buffer was added continuously over 2 h until the gel was swollen and covered with buffer. The gel was then incubated with trypsin overnight at 37°C.

Peptides were extracted onto Ziptips (Millipore) from an aliquot of the solution and then washed with 0.1% trifluoroacetic acid (Applied Biosystems) and eluted directly to a matrix-assisted laser desorption ionization (MALDI) plate with 0.5 µl of 50% acetonitrile and 0.1% trifluoroacetic acid. The eluate was partially dried, and then 0.5 µl of alpha-cyano-4-hydrozycinnamic acid (Agilent) (5 mg/ml) was added. MALDI-mass spectrometry (MS) was performed using the reflector mode to obtain mono-isotopic peptide masses and tandem MS. The results were then used to search protein and genomic databases with the Mascot software. Further details are given in Bechtel et al [31].

EPR spectroscopy: Samples for X-band EPR spectroscopy were prepared in 3.8 mm thin walled precision quartz EPR sample tubes (Wilmad Lab Glass) by freezing anaerobically-prepared, buffered protein solutions with 20% (v/v) of 4 M sucrose as a glassing agent in liquid nitrogen and capping the tubes immediately. The frozen samples were stored in liquid nitrogen.

All EPR spectra were measured at the CalEPR Center at the University of California, Davis. Continuous-wave (CW) X-band spectra were acquired with an E-500 spectrometer (Bruker, Billerica, MA) under non-saturating slow-passage conditions using a Super-High Q resonator (ER 4122SHQE). Cryogenic temperatures were achieved and maintained using an Oxford Instruments ESR900 liquid helium cryostat in conjunction with an Oxford Instruments ITC503 temperature and gas-flow controller. Spectral simulations were performed with Matlab using the

EasySpin 4.0 toolbox [32]. Quantitation of the concentration of $S = 1/2$ spin systems in the vicinity of $g = 2$ concentration within a sample was achieved by comparing the double integral of the EPR intensity to that of a 308 μM Cu(II) in 100 mM EDTA (EDTA = ethylenediaminetetraacetic acid) at pH 7 spin-standard [33]. All data were corrected for differences in incident microwave power, acquisition temperature, and cavity quality factor. All concentrations are given in μM.

Detection of Co(I) and Co(II) cobalamins by electronic absorption spectroscopy: Enzyme-bound Cob(I)alamin was detected in VcrA-MBP by the UV-Vis absorption at 385 nm (388 nm for VcrA) and 555 nm (550 nm for VcrA) and estimated by the measured extinction coefficients of 22 $mM^{-1}cm^{-1}$ at 385 or 388 nm and 9 $mM^{-1}cm^{-1}$ at 550 or 555 nm. For the detection of the enzyme-bound Cob(II)alamin, the absorbance at 475 nm was monitored (ε = 9.47 mM^{-1} cm^{-1} at 477 nm [34]). The spectra were measured on an Ultrospec 2100 Pro® UV-visible spectrophotometer (Amersham Biosciences) in cuvettes of 1 cm path length.

Synthesis and purification of aquahydroxocobinamide [(H_2O)OHCbi]: 10 mg of $(CN)_2$Cbi or dicyanocobinamide (Sigma Aldrich) whose UV-visible spectrum was identical to the reported spectrum[35,36], was dissolved in 3 ml anaerobic 0.1 M NaOH, and small aliquots of sodium borohydride pellets were added every 5 minutes, until a molar excess of about 10-fold of borohydride over $(CN)_2$Cbi was reached. The reaction proceeded for about 1.5 h until the mixture was tranferred into a beaker and quenched by the addition of acidified water. The final pH was adjusted to 3 and the mixture was purified over a 1 g Sep Pak C_{18} reverse phase column (Waters). The column was pre-conditioned prior to sample loading by washing once with 100% methanol and five times thereafter with 0.1% (v/v) TFA (trifluoroacetic acid). After the sample had passed through the column, salts were removed by washing with 0.1% TFA for five column volumes. This was followed by elution with 100% methanol, and the collected orange fractions were evaporated overnight at room temperature. The collected product (6 mg) was identified as (H_2O)OHCbi by its UV-visible absorption spectrum which was identical to the spectrum reported in the literature[35,36].

RESULTS AND DISCUSSION

Overproduction, reconstitution, and specific activities: 3-5 mg of MBP-tagged VcrA-MBP was produced from 3 g of cells (wet weight). VcrA, as isolated from *Dehalococcoides mccartyi* strain VS, was shown previously to contain molar ratios of Fe and S consistent with a stoichiometry of two [4Fe-4S] clusters as well as one corrinoid cofactor per enzyme; the monomeric enzyme is membrane-associated putatively via a small integral membrane protein (VcrB) facing the outside [10,16] (see Fig S1). Heterologous overproduction of VcrA-MBP from plasmid pLIC-HMK resulted in the formation of inclusion bodies, and all VcrA-MBP was found in the insoluble fraction (data not shown). No significant soluble VcrA-MBP was observed upon increasing the induction time beyond 3 h, or by varying the growth medium between several rich (LB, Standard I, TB) or minimal media containing glucose, the growth temperatures from 16-37°C, the host *E. coli* strain (BL21, BL21 DE3, BL21pLys) or the inducer concentration between 50-1000 μM (data not shown). Therefore, VcrA-MBP was purified from inclusion bodies under denaturing conditions to apparent homogeneity using His-tag affinity chromatography. Using a Ni-IDA matrix column, nearly homogenous protein was obtained (Fig 1). Subsequently, the denatured protein was desalted in the presence of 20% glycerol and 0.2% CHAPS followed by refolding and reconstitution of the cobalamin and iron-sulfur cluster cofactors. Excess cofactors were removed, and metal analysis (via ICP-MS and spectrophotometric estimation) was performed, indicating a 1-1.4 mol Co and 8-12 mol non-heme iron ratio per mol purified VcrA-MBP. When reconstituted VcrA (see below) was subjected to the same analysis, a Co content of 0.8-1.1 mol and a non-heme iron content of 7-10 mol per mol of purified enzyme was found.

Heterologously produced and cofactor-reconstituted VcrA-MBP catalysed the reduction of vinyl chloride, 1,1-DCE, *cis* and *trans* 1,2-DCE at high specific activities (Table 1). Vinyl chloride was reductively dehalogenated to ethene at a V_{max} of 1050 nmol*min^{-1}*[mg protein]$^{-1}$ and a K_M of 10 μM, which is very similar to the specific activity of the purified, native VcrA (990 nmol*min^{-1}*[mg protein]$^{-1}$, for which a K_M was not reported [10]. Also, 1,1-DCE was dehalogenated to vinyl chloride and ethene at a V_{max} of about 295 nmol*min^{-1}*[mg protein]$^{-1}$ (K_M = 50 μM), (Table 1, Fig 2a). 1,1-DCE undergoes a two-step conversion into ethene via vinyl chloride as intermediate and does not follow Michaelis-Menten behavior below 10 μM (data not

shown). 1,1-DCE in native VcrA proceeded at a V_{max} of 390 nmol*min^{-1}*[mg protein]$^{-1}$ [10]. When testing as an abiotic control coenzyme B_{12} at equivalent molar concentration but without VcrA in the assay, a slow rate of vinyl chloride reduction of 100 nmol/min was observed (data not shown). For 1,1-DCE dehalogenation, the maximum abiotic dechlorination rates were about 25 nmol/min, which is less than 10% of the enzymatic rate, at B_{12} concentrations comparable to those present in the enzyme.

Interestingly, VcrA-MBP was also found to mediate the dihaloelimination of 1,2-DCA to ethene (Table 1; Fig 2b). This is a novel activity and was not previously observed. The maximum specific activity of complete 1,2-DCA dehalogenation by VcrA-MBP was 450 nmol*min^{-1}*[mg protein]$^{-1}$ (Table 1). However, the K_M of 1300 μM is 2 orders of magnitude higher than for vinyl chloride or 1,1-DCE, suggesting that 1,2-DCA may not be a physiological substrate *in situ* for VcrA. This extended substrate specificity of VcrA has implications for chlorinated solvent-contaminated sites, which contain both chloroethanes and chloroethenes. *Dehalococcoides* VS could be expected to consume 1,2-DCA faster than vinyl chloride, 1,1- or the 1,2-DCE isomers, but only if the initial concentration of the former is much higher than those of the chloroethenes and higher than those encountered in most natural environments. It is unclear whether 1,2-DCA dihaloelimination is also coupled to energy conservation *in vivo*. However, 1,2-DCA is also far more water-soluble (up to 100 mM) than the chloroethenes; so the actual dechlorination rates in the environment may be different from what the Michaelis-Menten parameters predict.

Methyl viologen-independent dehalogenation: Consistent with previous *in vitro* dehalogenation studies[37,38], the presence of methyl viologen for reductive dehalogenation activity of VcrA-MBP was not essential, although a methyl viologen-induced acceleration of the reaction rates was observed. Methyl viologen-independent dehalogenation rates in this case were about 20-25% of the rates in the presence of methyl viologen (Table 1).

Interestingly, upon removal of the MBP tag via proteolytic cleavage, the purified and cofactor-reconstituted VcrA also showed dehalogenation activity regardless of whether methyl viologen was absent or present. The methyl viologen-independent rates were 45-55% of the rates observed in the presence of methyl viologen (Table 1). The fact that methyl viologen accelerates the rates of dechlorination both in VcrA-MBP and VcrA suggests that it could create a chemical short cut

for transferring electrons directly of Co(II) to form the catalytically active Co(I) species, but the actual rates further depend on steric factors based on the conformation of the enzyme.

EPR studies: X-band CW EPR spectra of VcrA-MBP and VcrA were recorded under different reducing conditions. In the presence of 2 mM 2-mercaptoethanol, the observed EPR spectrum (top trace) of VcrA-MBP was nearly axial with *g*-values = [2.29, 2.23, 2.004] (blue trace, Fig 3A). The octet centered about $g_{\|}$ = 2.004 results from the splitting of the resonance due to the hyperfine interaction of the unpaired electron with the I = 7/2 ^{59}Co nucleus (100% natural abundance); $A_{\|}(^{59}\text{Co})$ = 305 MHz. Each of these lines was further split into a triplet due to an additonal hyperfine interaction with a single I = 1 ^{14}N nucleus ($A_{\|}(^{14}\text{N})$ = 52 MHz). These EPR spectral features are consistent with their assignment to a Cob(II)alamin species for which either the pendant dimethylbenzimidazole (DMB) is bound axially to the cobalt centre, or this DMB base has been replaced by some other nitrogenous ligand such as a histidine side chain from the polypeptide.

The CW EPR spectra of VcrA-MBP reconstituted with either aquahydroxocobinamide or dicyanocobinamide are essentially identical to one another, but markedly different from the spectrum of the cobalamin-reconstituted enzyme (Fig S4). The g-values move slightly upfield and the ^{14}N ligand hyperfine is lost the when the enzyme is reconstituted with cobinamide instead of cobalamin. This indicates that the dimethylbenzimidazole base of the cobalamin is likely serving as a ligand to the VcrA-bound cofactor, not a proteinaceous histidine ligand as in methionine synthase. Recent studies showed that dimethylbenzimidazole was essential for *D. mccartyi* dehalogenation[39], unlike in *Sulfurospirillum*-type microorganisms where the lower ligand is an adenine derivative. Therefore, our use of a dimethylbenzimidazole-containing corrinoid is relevant.

Further treatment of VcrA-MBP with the strong reductant Ti(III)-citrate left the Cob(II)alamin signal unchanged; however, a new intense signal appeared at *g* = [1.969, 1.928, 1.852] in the low-temperature EPR spectrum (Fig 3A, green trace). This new signal relaxed too quickly to be observed at temperatures above 60 K (Fig S5), which is consistent with the behaviour of reduced [4Fe-4S] clusters. Integration of the individual EPR signals revealed that approximately 69% of the total signal corresponded to reduced [4Fe-4S] centers and the 31% of the EPR spectrum

corresponded to Cob(II)alamin, in line with the elemental analysis showing 1-1.4 Co mol and 8-12 mol non-heme iron per mol of enzyme (Table S1).

An additional signal appeared at g = [1.989, 1.928, 1.900] that varied in intensity with each preparation (Fig 3B). This new signal was greatly diminished following an additional rapid desalting step (via a 10 kDa cut-off Centricon membrane filter) in the sample preparation (Fig S6) and looked similar to signals measured recently for Ti(III)-containing compounds [40]. Thus, we concluded that the features at [1.989, 1.928, 1.900] arise from S = 1/2 Ti(III) species generated during the reduction.

Interestingly, though Ti(III)citrate should be a sufficiently strong reductant to reduce Cob(II)alamin to Co^{1+}, it seems insufficient to do so for cobalamin bound to VcrA-MBP. Only upon further addition of methyl viologen did the Cob(II)alamin EPR spectrum disappear. The intensity of the $[4Fe\text{-}4S]^{+}$ signal was unchanged (Fig 3B). This spectral change coincided with the appearance of new features at ≈385 nm and ≈555 nm in the electronic absorption spectrum that is indicative of Cob(I)alamin. Samples of Ti(III)-citrate and methyl viologen reduced VcrA with 1,1-DCE as a substrate or with 50 μM iodoacetamide as an inhibitor did not change the spectra substantially (data not shown). The EPR spectra of the Ti(III)-reduced, cobalamin-reconstituted VcrA are similar to those of VcrA-MBP. Specifically, we observe signals from Co(II)Cbl (not shown) as well as signals from two reduced [4Fe4S] clusters and adventitious Ti(III) species (Fig S7). Both FeS cluster signals observed in samples of VcrA lacking the MBP tag possess slightly different g-tensors than that determined for the FeS cluster in the samples of VcrA-MBP. The origin of these differences is unclear at this time. However, subtle changes in g-values are expected if the MBP tag influences the structure of VcrA. Second-coordination sphere interactions are well-known to modulate EPR properties of FeS clusters. Additionally, it is possible that in these samples both clusters in VcrA (two [4Fe-4S] clusters being suggested by iron content analysis) are reduced and in sufficiently close proximity to one another so as to cause a shifting of some of the resonant field positions due to through-space spin-dipole interactions. This hypothesis will be evaluated in the future using multifrequency EPR techniques.

The intensity of the Cob(II)alamin signal was reduced by approximately 70% upon oxidation by the presence of 10 mM ferricyanide (Fig 4). Upon addition of up to 50-75 mM ferricyanide, the Co(II) signal was completely abolished (data not shown) and no new signals appeared except for a broad derivative feature, that was also present in spectra of samples containing only 1 mM ferricyanide. Chemical oxidation in the absence of molecular oxygen yielded oxidized [4Fe-4S] cluster(s) and oxidized cobalamin that are both EPR silent. No EPR evidence for oxidized [3Fe4S] clusters was found in the ferricyanide-treated samples[41].

UV-visible spectrophotometry: Titration of VcrA-MBP with Ti(III)-citrate up to concentrations of 1.6 mM reduced the intensities of the iron-sulfur signal (420 nm) and produced peaks at 385 and 475 nm (Fig S8, panel A). Estimation of the Cob(I)alamin vs. Cob(II)alamin using the reported extinction coefficients (see methods section) showed only about 10% of the cobalamin in the Co(I) state. However, if 0.4 mM methyl viologen was added to VcrA-MBP, then the sequential titration with Ti(III)-citrate produced increasing absorption of three sharp peaks at 366 nm, 385 nm, characteristic of the Co(I) state (Fig S8, Panel B), and 395 nm. A broad peak also appeared for reduced methyl viologen at 600 nm, and the intensity of the peak for Co(I) around 555 nm increased (Fig S8, panel B). The spectrum of free methyl viologen and Ti(III)-citrate overlaps considerably with that of VcrA-MBP reduced with methyl viologen and Ti(III)-citrate from 350- 450 nm, and is quite different from that of the unreduced enzyme (Fig S8, panel C). Further, Cob(I)alamin also spontaneously reoxidizes to the Co(II) state. This makes the accurate quantification of Cob(I)- vs Cob(II)alamins in the methyl viologen-reduced enzyme difficult. However, VcrA-MBP undergoes a shift of a peak from 530 nm for Co(II) to 555 nm typical for Co(I) upon reduction; we estimated about 70-90% of the cobalamin must be in the Co(I) state based on the absorption at 555 nm (calculated extinction 9.0 mM^{-1} cm^{-1}).

In contrast, VcrA (lacking MBP) exhibited quite different UV-vis spectroscopic features upon reduction by Ti(III)-citrate (Fig S9, Panel A). An intense peak at 388 nm characteristic of Cob(I)alamin and a smaller peak at 550 nm appeared 1 mM Ti(III) in the absence of methyl viologen. Concomitant with the appearance of the Cob(I)alamin signal, the 475 nm Cob(II)alamin maximum was replaced by another at 465 nm (which shows that cobalamin is still

bound to VcrA). The spectra measured in this experiment are strikingly similar to those of the corrinoid iron sulfur protein[42] where Co(I)corrinoid species also play a key catalytic role.

Based on the extinction coefficients estimated in our study, we calculated that about 99% of the enzyme-bound cobalamin was reduced to the Co(I) state at approximately 1.5 mM of Ti(III). The methyl viologen mediated spectra of VcrA were similar to those of VcrA-MBP with methyl viologen (Fig S9, Panel B). The disappearance of the Co(II)Cbl signal as assessed by EPR spectroscopy is correlated to the appearance Co(I)Cbl features in the UV-visible spectrum, demonstrating the presence of Co(I)Cbl in the catalytically competent form of VcrA.

CONCLUSIONS

We have established a heterologous platform to produce the VcrA enzyme, which can be reconstituted in the fully active form. This is also the first biochemical report to unambiguously demonstrate the existence of a bifunctional chloroethene and chloroethane reductive dehalogenase. This observation has strong implications for the remediation of sites co-contaminated with chloroethenes and chloroethanes.

Interestingly, although the exact chemical identity of the corrinoid cofactor of native VcrA is unknown, heterologously expressed VcrA-MBP reconstituted with hydroxocobalamin or adenosylcobalamin has kinetic properties that are indistinguishable from that of native VcrA. Since we did not use dark/red light conditions, the active species was likely to be hydroxocobalamin. The use of either cobalamin derivative did not lead to any difference in the specific activity (data not shown). Based on the findings reported here we propose that native VcrA coordinates Cob(II)alamin with an ^{14}N axial ligand, which arises most likely from the dimethylbenzimidazole moiety of the cofactor. Earlier corrinoid cross-feeding studies[8] suggested that dimethylbenzimidazole (DMB), the lower ligand of cobalamins was essential for the reductive dechlorination of chloroethenes by defined microbial consortia containing *D. mccartyi*, which is consistent with our findings. Base-on cobalamins were reported to have Co(II)/Co(I) reduction potentials of about -600 mV (SHE) while base-off cobalamins potentials are around -500 mV [43]. The exact potential of the Co(II)/Co(I) couple depends on the interaction of the cobalamin with the polypeptide. The [4Fe-4S] clusters which are reducible by Ti(III) *in vitro*

may be reduced *in vivo* possibly by ferrdoxin/flavodoxin. We can distinguish only one class of EPR signals associated with the reduced [4Fe-4S] clusters. Thus, the two putative clusters are either spectroscopically equivalent or we are only able to observe one of two classes under our experimental conditions. Furthermore, these clusters do not necessarily have different reduction potentials. A chemical model study of the dehalogenation of chloroethenes reported a reduction potential in free solution of -450 mV for the vinyl radical with much more positive potentials for the chloroethyl radicals [44]. Thus, a mechanism where a Cob(I)alamin species donates an electron to the chlorinated compound, leading to radical dechlorination (Fig 5) may be envisaged. The vinyl-type radical could be finally reduced by either a [4Fe-4S] cluster (as in Fig 5B) or a second Co(I) (as in Fig 5A) and protonated to yield the product.

The recently published crystal structures of PCE dehalogenase [45] and of NpRdhA[18] seem to lend support to our mechanism. The mechanism is similar to the one proposed by Ragsdale and others for the dehalogenation of 3-chloro-4-hydroxy benzoic acid [46]. While the proposed mechanism serves as a basis for future experiments with recombinant VcrA, our studies reported here provided novel insights into an environmentally important *Dehalococcoides*-type reductive dehalogenase.

ACKNOWLEDGEMENTS: Funding for this work was provided by ENI and NSF to AMS and by the National Institutes of Health to (GM-104543) RDB. We thank Dick Winant (PMF at the PAN Center, Stanford), Guangchao Li (ICP-MS at the School of Earth Sciences, Stanford), and Koshlan Meyer-Blackwell and Maeva Fincker for helpful discussions. We thank Maeva Fincker also for critically reading the manuscript and useful comments.

SUPPORTING INFORMATION AVAILABLE: The figures S1-S9 and table S1 are available free of charge via the Internet at http://pubs.acs.org.

FIGURES

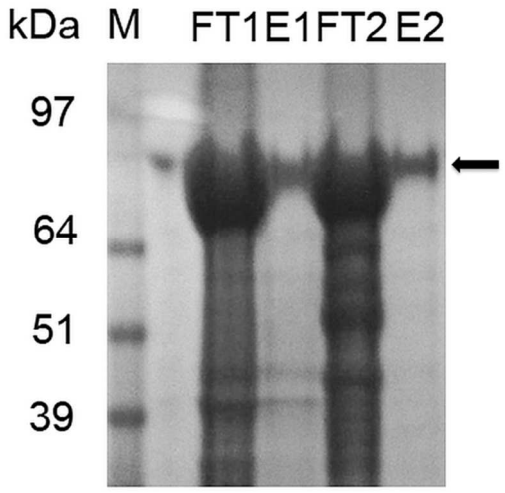

Fig 1. SDS-PAGE of VcrA-MBP purified by Ni-TED and Ni-IDA His-tag affinity chromatography columns under denaturing conditions. The arrow indicates the band corresponding to purified VcrA-MBP. M is the molecular mass marker. FT = flow through from the column and E = elution with 250 mM imidazole. Sample 1 was processed with a Ni-TED column and sample 2 with a Ni-IDA column.

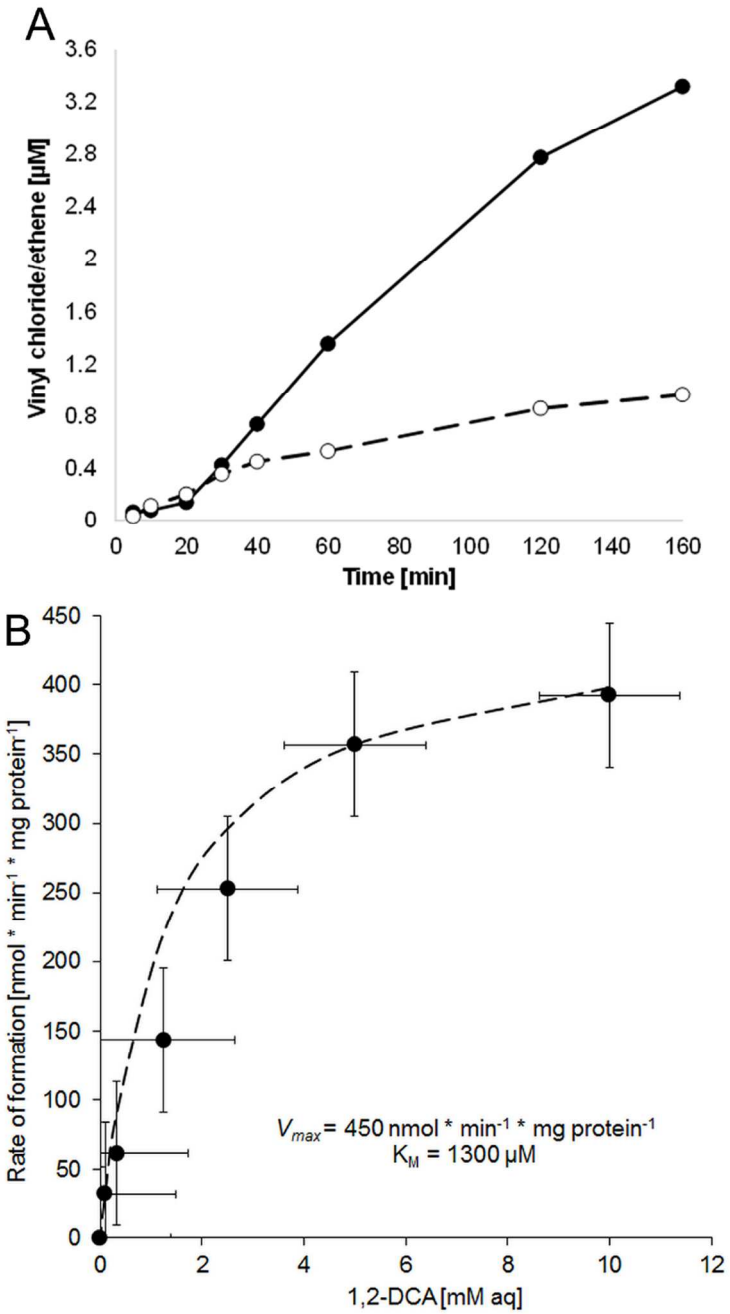

Fig 2. A). Reduction of 1,1-DCE to vinyl chloride (VC, empty circles) and ethene (Et, filled circles) by VcrA-MBP. The curve fitting suggests that the formation of both products follows second-order kinetics. **B)** Kinetics of 1,2 DCA dihaloelimination to ethene by VcrA-MBP. The Michaelis-Menten parameters were estimated as K_M = 1300 µM and *Vmax* = 450 nmol*min-

^{1}*[mg protein]$^{-1}$. The filled circles are the measured data points, while the dotted line represents the simulation based on the Michaelis-Menten equation. The cross-marks represent error bars.

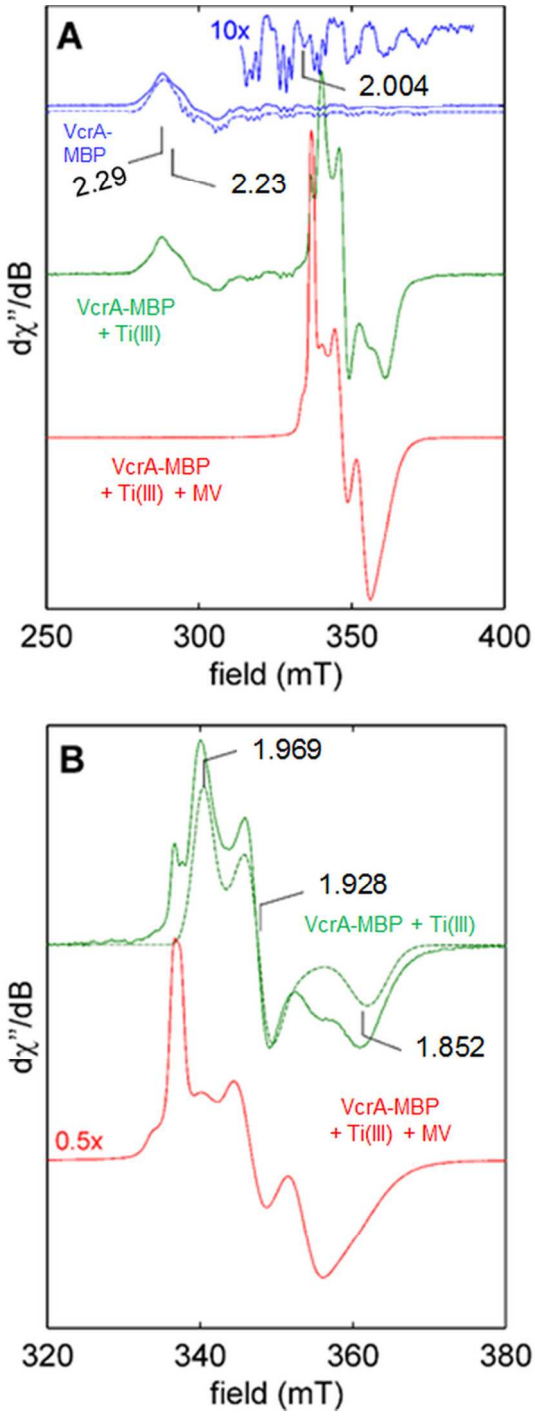

Fig 3 A. X band (9.367 GHz) EPR spectra of VcrA-MBP at 15 K under different reducing conditions. (Top) 2-mercaptoethanol-reduced VcrA-MBP (solid blue trace) with corresponding simulation (dashed blue trace) along with 10-fold magnification of features centered at g = 2.00

to better illustrate the ^{14}N hyperfine splitting. Ti(III)-reduced VcrA-MBP (middle, green trace) and Ti(III)-reduced VcrA-MBP following addition of methylviologen (bottom, red trace) are also shown. The *g*-values are indicated in the figure. Simulation parameters for the Cob(II)alamin species are as follows: g = [2.29, 2.23, 2.004]; g-Strain = [0.05, 0.04, 0.002]; $A(^{59}\text{Co})$ = [50, 40, 305] MHz; $A(^{14}\text{N})$ = [5, 5, 52] MHz). Spin quantification of the difference spectrum from the green and blue traces showed that the FeS signals: cob(II)alamin ratio is approximately 2:1 (77:34) (See Table S1).

B. Expansion of EPR spectrum of Ti(III)-reduced VcrA-MBP (top, solid green trace) and corresponding simulation of the $[4Fe\text{-}4S]^{+}$ contribution (dotted green trace) compared to the spectrum of Ti(III)-reduced VcrA-MBP following addition of methylviologen (red trace). Simulation parameters for the $[4Fe\text{-}4S]^{+}$ species are as follows: g = [1.969, 1.928 1.851]; g-Strain = [0.017, 0.018, 0.028].

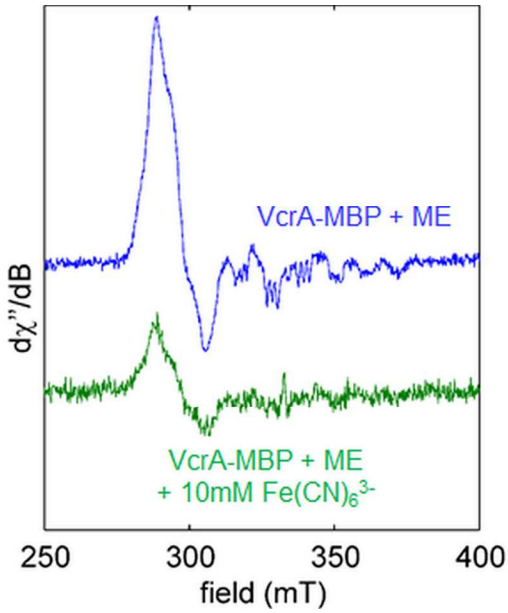

Fig. 4 Chemical oxidation in the absence of oxygen of 2-mercaptoethanol reduced VcrA-MBP: The top trace shows the X-band EPR spectrum VcrA-MBP reduced with 2-mercaptoethanol, whereas the bottom trace shows the same sample treated with 10 mM ferricyanide. The intensity of the Cob(II)alamin signal is reduced by about 70%; upon the further addition of ferricyanide (50-75 mM) the signal is completely abolished (data not shown). No [3Fe-4S] signals were observed.

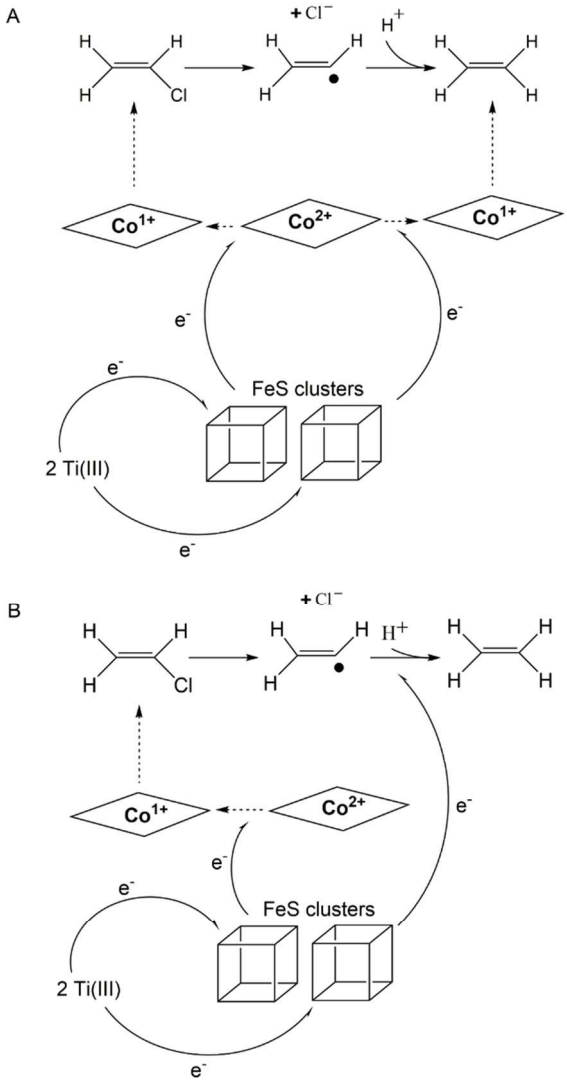

Fig 5. Proposed reaction mechanism(s) for reductive dehalogenation by VcrA; Co(II) is reduced to Co(I) by a low potential ferredoxin/flavodoxin physiologically or Ti(III) *in vitro*. Co(I) donates an electron to the substrate eliminating Cl^- and generating a substrate radical; this radical is further reduced by an electron originating either from a second Co(I) as in Scheme A or directly by a [4Fe-4S] cluster as in Scheme B; protonation possibly simultaneous to the second reduction, leads to the formation of the product. Vinyl chloride is shown as the substrate here, but the same mechanism could dechlorinate 1,1-DCE and other substrates.

Table 1 Substrates tested in this study for transformation by VcrA and VcrA-MBP, and their Michaelis-Menten parameters. VcrA = enzyme without MBP and His tags; VcrA-MBP = enzyme with His and MBP tags intact. MV = methyl viologen.

Substrate	VcrA-MBP (molar mass 100 kDa)					VcrA, no MBP (molar mass 57 kDa)				
	V_{max} [nmol*min^{-1}*(mg protein)$^{-1}$] with MV	K_{cat} [s^{-1}] with MV	Vmax [nmol*min-1*(mg protein)-1] without MV	K_{cat} [s^{-1}] without MV	K_M [μM]	V_{max} [nmol*min^{-1}*(mg protein)$^{-1}$] with MV	K_{cat} [s^{-1}] with MV	V_{max} [nmol*min^{-1}*(mg protein)$^{-1}$] without MV	K_{cat} [s^{-1}] without MV	K_M [μM]
1,1-DCE	295	177	73	43.8	50	675	578	300	257	45
VC	1050	630	265	159	10	2250	1928	1006	862	13
1,2-DCA	450	270	80	96	1300	722	618	395	338	1300

REFERENCES

(1) Squillace PJ; Moran MJ; Lapham W; Price C; Clawges R; Zogorski JS *J Environ Sci Technol* **1999**, *33*, 4176.
(2) Sutfin JA *International Groundwater Technol* **1996**, *2*, 7.
(3) US EPA, T. I. O. *Bioremediation of chlorinated solvent contaminated groundwater*, 1998.
(4) Golding BT; Anderson RA; Ashwell S; Edwards CH; Garnett I; Kroll F; Buckel W In *Vitamin B12 and B12-proteins*; Kräutler B, Arigoni D, Golding BT, Eds.; Wiley-VCH: Weinheim, 1998, p 209.
(5) Sjuts H; Fisher K; Dunstan MS; Rigby SE; Leys D *Protein Exp Purif* **2012**, *85*, 224.
(6) Schmitz RPH; Habel A; Ploss K; Boland W; Wolf J; Neumann A; Svatos A; Diekert G *Environ Sci Technol* **2007**, *41*, 7370.

(7) van de Pas BA; Smidt H; Hagen WR; van der Oost J; Schraa G; Stams AJM; de Vos WM *J Biol Chem* **1999**, *274*, 20287.
(8) van de Pas BA; Gerritse J; de Vos WM; Schraa G; Stams AJM *Arch Microbiol* **2001**, *176*, 165.
(9) Magnuson JK; Romine MF; Burris DR; Kingsley MT *Appl Environ Microbiol* **2000**, *66*, 5141.
(10) Mu̅ller JA; Rosner BM; von Abendroth G; Meshulam-Simon G; McCarty PL; Spormann AM *Appl Environ Microbiol* **2004**, *70*, 4880.
(11) Grostern A; Edwards EA *Appl Environ Microbiol* **2009**, *75*, 2684.
(12) Marzorati M; Balloi A; de Ferra F; Corallo L; Carpani G; Wittebolle L; Verstraete W; Daffonchio D *Microbial Cell Factories* **2010**, *9*, 1.
(13) Schumacher W; Holliger C *J Bacteriol* **1996**, *178*, 2328.
(14) Louie TM; Mohn WW *J Bacteriol* **1999**, *181*, 40.
(15) Miller E; Wohlfarth G; Diekert G *Arch Microbiol* **1996**, *166*, 379.
(16) Rosner BM; Spormann AM; McCarty PL *Appl Environ Microbiol* **1997**, *63*, 4139.
(17) Mac Nelly A; Kai M; Svatoš A; Diekert G; Schubert T *Appl Environ Microbiol* **2014**, *80*, 4313.
(18) Payne KAP; Quezada CP; Fisher K; Dunstan MS; Collins FA; Sjuts H; Levy C; Hay S; Rigby SEJ; Leys D *Nature* **2014**, published online.
(19) Sambrook J; Maniatis T; Fritsch EF *Molecular cloning: a laboratory manual*; Cold Spring Harbor Laboratory: New York, 1989; Vol. 1 & 2.
(20) Doyle SA *Methods Mol Biol* **2005**, *310* 107.
(21) Kapust RB; Waugh DS *Protein Sci* **1999**, *8*, 1668.
(22) Corn JE; Pease PJ; Hura GL; Berger JM *Mol Cell* **2005**, *20*, 391.
(23) Studier FW *Protein Exp & Purif* **2005**, *41*, 207.
(24) Anspach FB *J Chromato A* **1994**, *672*, 35.
(25) Hemdan ES; Porath J *J Chromato* **1985**, *323*, 255.
(26) Smith FE; Herbert J; Gaudin J; Hennessy DJ; Reid GR *Clin Biochem* **1984**, *17*, 306.
(27) Fish WW *Methods Enzymol* **1988**, *158*, 357.
(28) Baker SA; Miller-Ihli NJ *Spectrochim Acta Part B* **2000**, *55*, 1823.
(29) Chen JH; Jiang SJ *J Agri Food Chem* **2008**, *56*, 1210.
(30) Freedman DL; Danko AS; Verce MF *Water Sci Technol* **2001**, *43*, 333.
(31) Bechtel JT; Winant RC; Ganem D *J Virol* **2005**, *79*, 4952.
(32) Stoll S; Schweiger A *J Magn Reson* **2006**, *178*, 42.
(33) Eaton GR; Eaton SS; Quine RW; Mitchell D; Kathirvelu V; Weber RT *J Magn Reson* **2010**, *205*, 109.
(34) Goulding CW; Postigo D; Matthews RG *Biochemistry* **1997**, *36*, 8082.
(35) Brodie JD *Proc Natl Acad Sci* **1969**, *62*, 461.
(36) Blackledge WC; Blackledge CW; Griesel A; Mahon SB; Brenner M; Pilz RB; Boss GR *Anal Chem* **2010**, *82*, 4216.
(37) Neumann A; Siebert A; Trescher T; Reinhardt S; Wohlfarth G; Diekert G *Arch Microbiol* **2002**, *177*, 420.
(38) Nijenhuis I; Zinder SH *Appl Environ Microbiol* **2005** *71*, 1664.
(39) Men Y; Seth EC; Yi S; Allen RH; Taga ME; Alvarez-Cohen L *Appl Environ Microbiol* **2014**, *80*, 2133.
(40) Maurelli S; Morra E; Van Doorslaer S; Busico V; Chiesa M *Phys Chem Chem Phys* **2014**, *16*, 19625.
(41) Liu A; Gräslund A *J Biol Chem* **2000**, *275*, 12367.
(42) Kung Y; Ando N; Doukov TI; Blasiak LC; Bender G; Seravalli J; Ragsdale SW; Drennan CL *Nature* **2012**, *484*, 265.
(43) Banerjee RV; Harder SR; Ragsdale SW; Matthews RG *Biochemistry* **1990**, *29*, 1129.
(44) Pratt DA; van der Donk WA *J Am Chem Soc* **2005**, *127*, 384.
(45) Bommer M; Kunze C; Fesseler J; Schubert T; Diekert G; Dobbek H *Science* **2014**, *346*, 455.

(46) Krasotkina J; Walters T; Maruya KA; Ragsdale SW *J Biol Chem* **2001**, *276*, 40991.

FOR TABLE OF CONTENTS USE ONLY

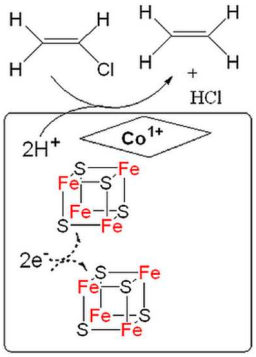

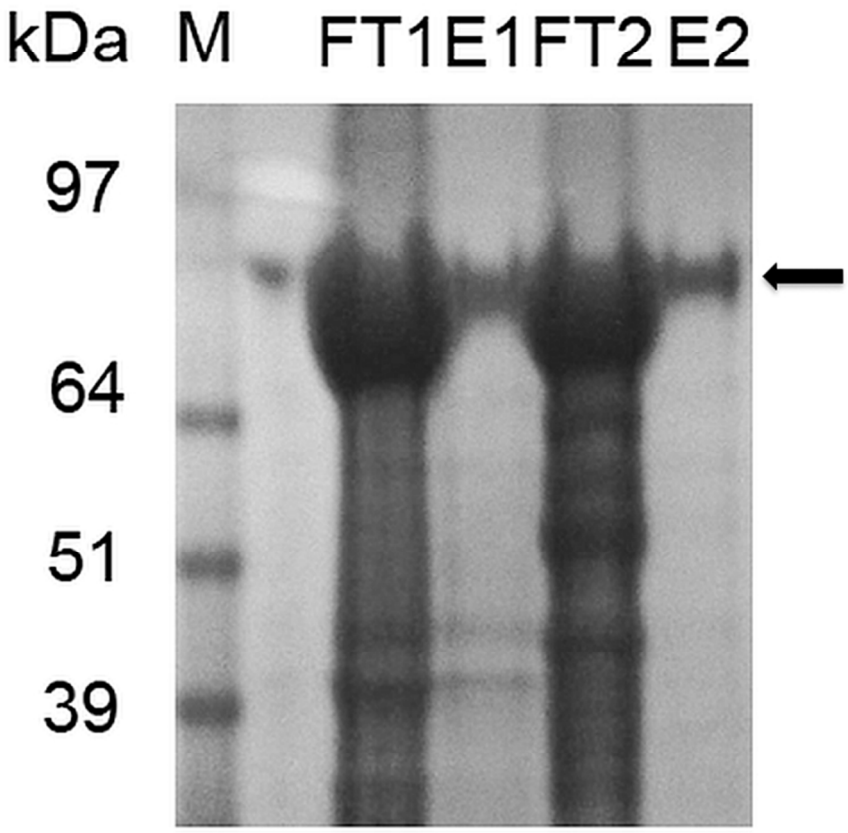

85x93mm (300 x 300 DPI)

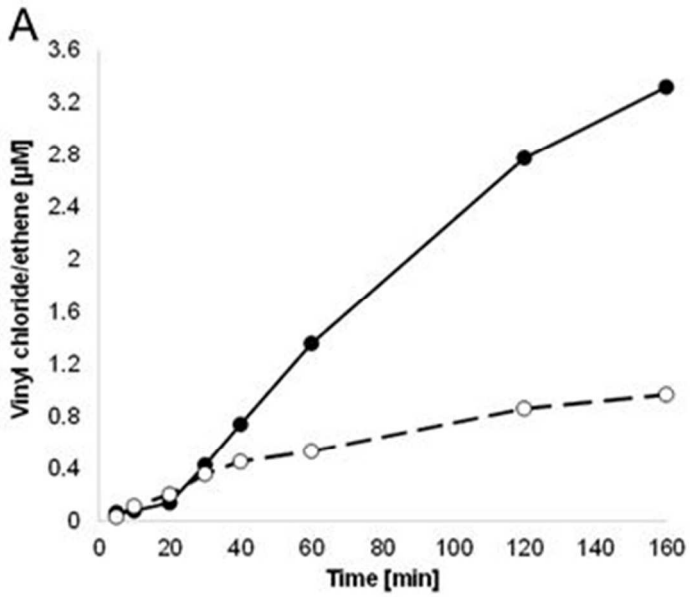
A
3.6
3.2
2.8
2.4
2
1.6
1.2
0.8
0.4
0
Vinyl chloride/ethene [µM]
0
20
40
60
80
100
120
140
160
Time [min]

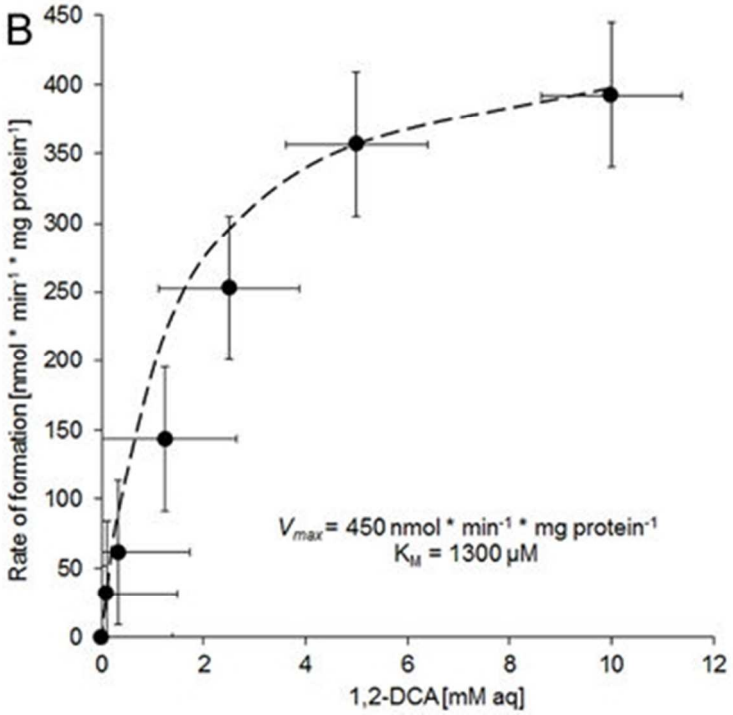
B
Rate of formation [nmol * min-1 * mg protein-1]
1,2-DCA [mM aq]
Vmax = 450 nmol * min-1 * mg protein-1
KM = 1300 µM
0
50
100
150
200
250
300
350
400
450
0
2
4
6
8
10
12

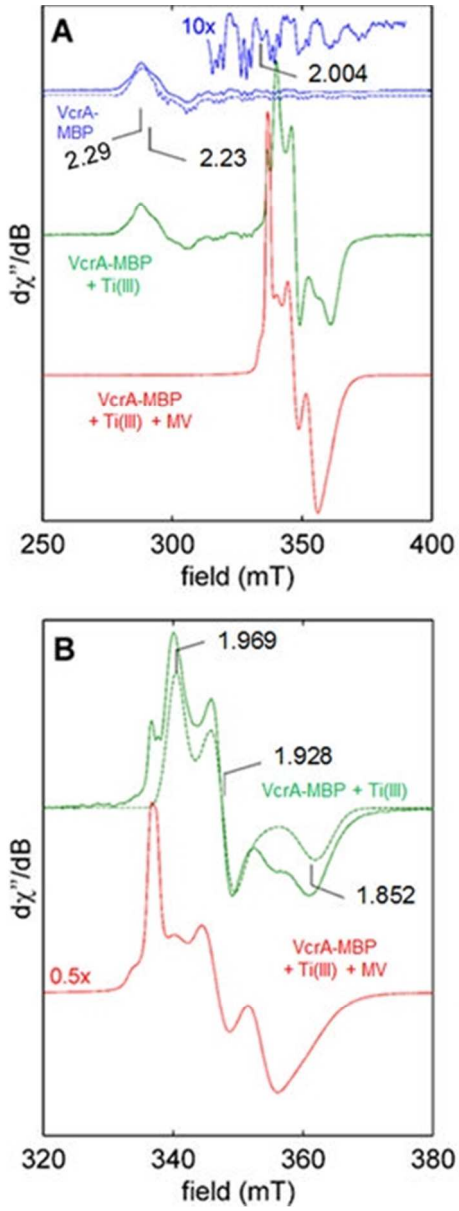
A
10x
2.004
VcrA-MBP
2.29
2.23
VcrA-MBP + Ti(III)
VcrA-MBP + Ti(III) + MV
dχ"/dB
250
300
350
400
field (mT)
B
1.969
1.928
VcrA-MBP + Ti(III)
1.852
VcrA-MBP + Ti(III) + MV
0.5x
dχ"/dB
320
340
360
380
field (mT)

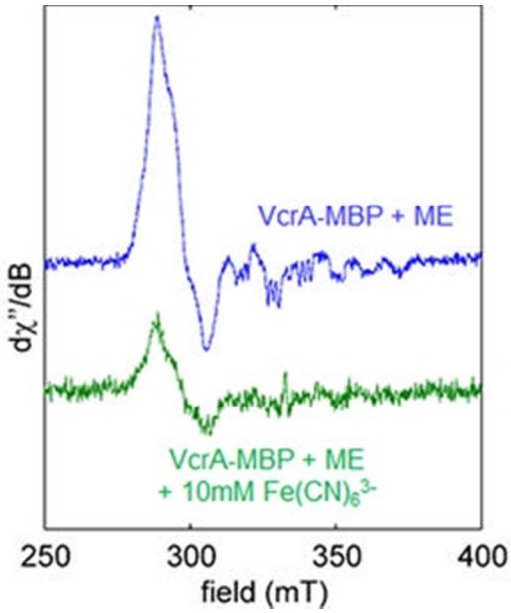
VcrA-MBP + ME
VcrA-MBP + ME
+ 10mM Fe(CN)6 3-
dχ''/dB
250
300
350
400
field (mT)

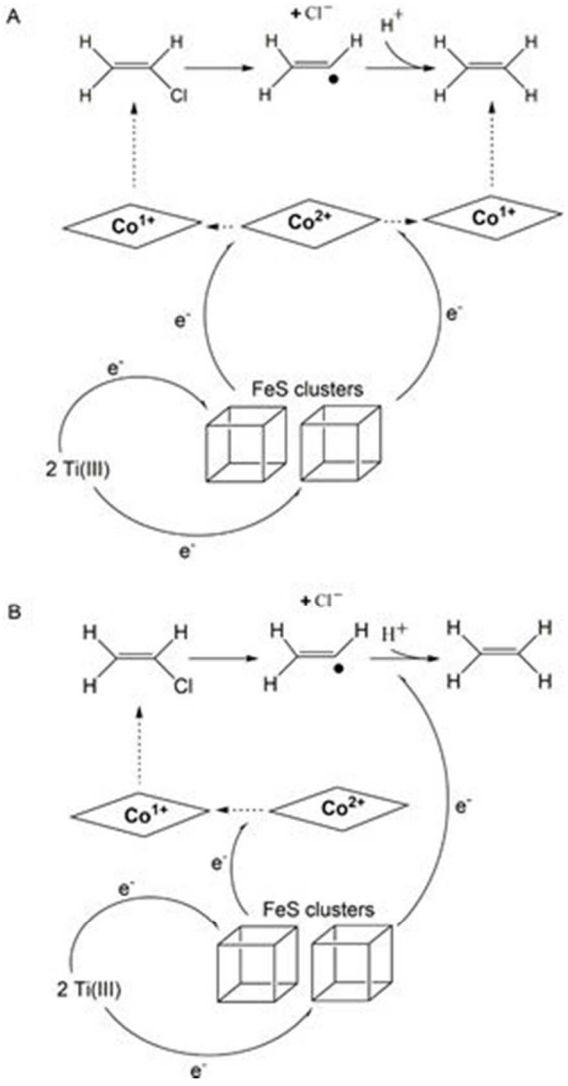
A
+Cl⁻
H⁺
Cl
Co1+
Co2+
Co1+
e⁻
e⁻
e⁻
FeS clusters
2 Ti(III)
e⁻
B
+Cl⁻
H⁺
Cl
Co1+
Co2+
e⁻
e⁻
e⁻
FeS clusters
2 Ti(III)
e⁻

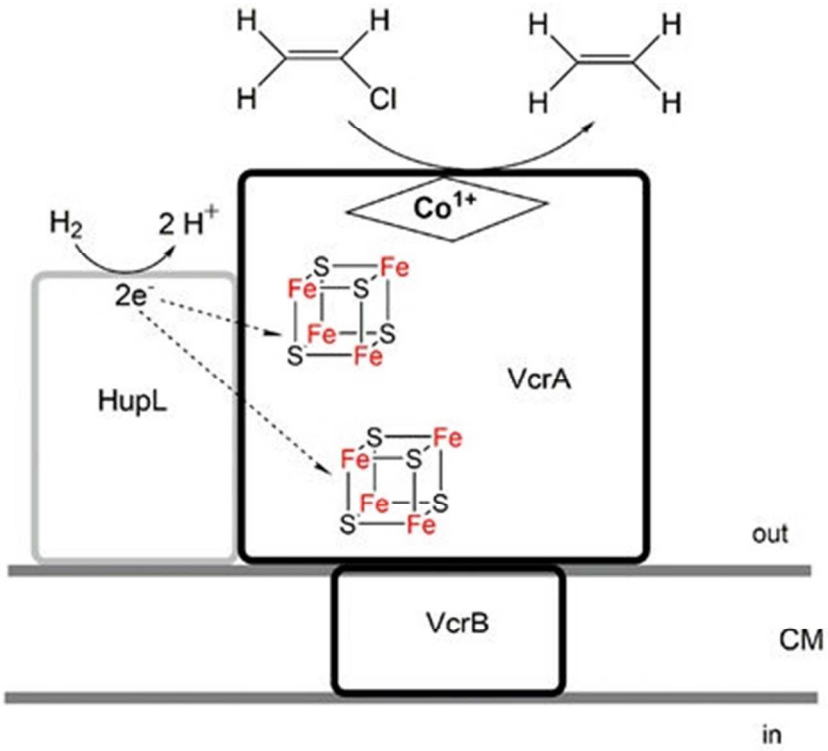
H
H
H
Cl
H
H
H
H
Co1+
H2
2 H+
2e-
HupL
VcrA
VcrB
out
CM
in

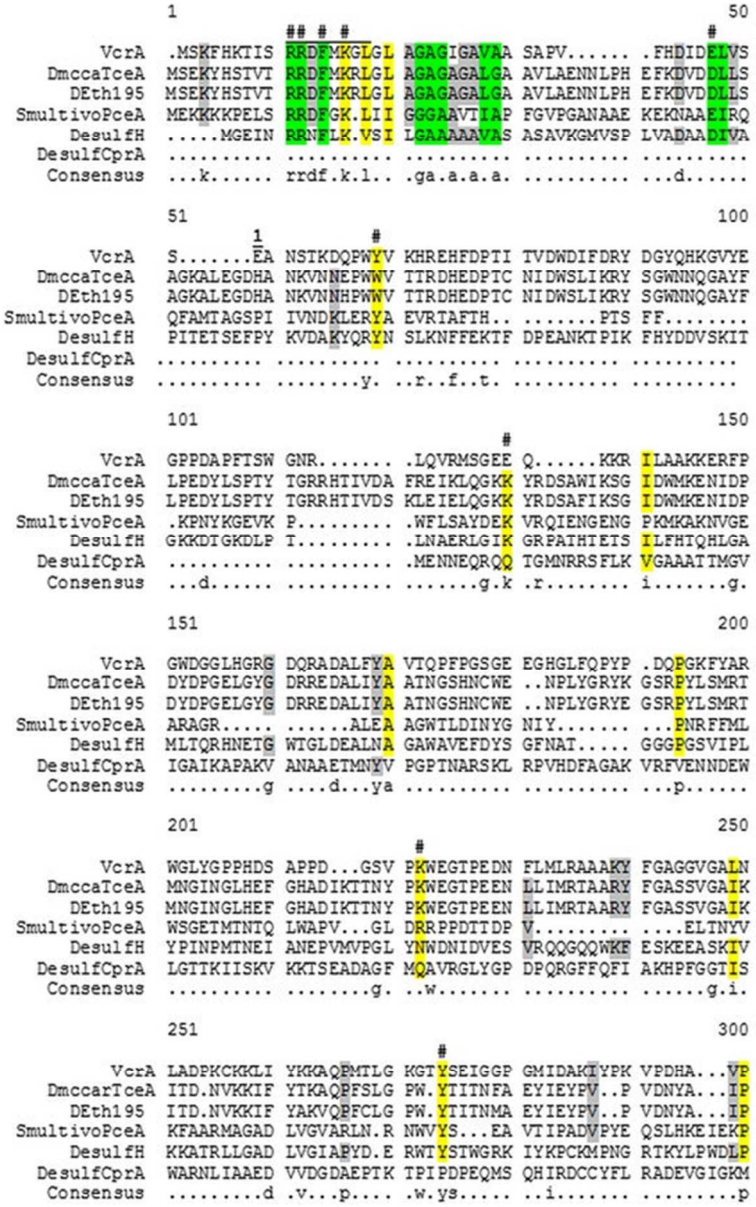
1 50
VcrA .MSKFHKTIS RRDFMKGLGL AGAGIGAVAA SAPV..... .FHDIDELVS
DmccaTceA MSEKYHSTVT RRDFMKRLGL AGAGAGALGA AVLAENNLPH EFKDVDDLLS
DEth195 MSEKYHSTVT RRDFMKRLGL AGAGAGALGA AVLAENNLPH EFKDVDDLLS
SmultivoPceA MEKKKKPELS RRDFGK.LII GGGAAVTIAP FGVPGANAAE KEKNAAEIRQ
DesulfH .....MGEIN RRNFLK.VSI LGAAAAAVAS ASAVKGMVSP LVADAADIVA
DesulfCprA ....
Consensus ...k..... rrdf.k.l.. .ga.a.a.a. ....d.....
51 100
VcrA S.....EA NSTKDQPWYV KHREHFDPTI TVDWDIFDRY DGYQHKGVYE
DmccaTceA AGKALEGDHA NKVNNEPWWV TTRDHEDPTC NIDWSLIKRY SGWNNQGAYF
DEth195 AGKALEGDHA NKVNNHPWWV TTRDHEDPTC NIDWSLIKRY SGWNNQGAYF
SmultivoPceA QFAMTAGSPI IVNDKLERYA EVRTAFTH.. .....PTS FF.....
DesulfH PITETSEFPY KVDAKYQRYN SLKNFFEKTF DPEANKTPIK FHYDDVSKIT
DesulfCprA ....
Consensus ....y. ..r..f..t. ....
101 150
VcrA GPPDAPFTSW GNR..... .LQVRMSGEE Q.....KKR ILAAKKERFP
DmccaTceA LPEDYLSPTY TGRRHTIVDA FREIKLQGKK YRDSAWIKSG IDWMKENIDP
DEth195 LPEDYLSPTY TGRRHTIVDS KLEIELQGKK YRDSAFIKSG IDWMKENIDP
SmultivoPceA .KPNYKGEVK P..... .WFLSAYDEK VRQIENGENG PKMKAKNVGE
DesulfH GKKDTGKDLP T..... .LNAERLGIK GRPAITHTETS ILFHIQHLGA
DesulfCprA .... .MENNEQRQQ TGMNRRSFLK VGAAATTMGV
Consensus ...d..... ....g.k .r..... i.....g.
151 200
VcrA GWDGGLHGRG DQRADALFYA VTQPFPGSGE EGHGLFQPYP .DQPGKFYAR
DmccaTceA DYDPGELGYG DRREDALIYA ATNGSHNCWE ..NPLYGRYK GSRPYLSMRT
DEth195 DYDPGELGYG DRREDALIYA ATNGSHNCWE ..NPLYGRYE GSRPYLSMRT
SmultivoPceA ARAGR..... .....ALEA AGWTLDINYG NIY..... ...PNRFFML
DesulfH MLTQRHNETG WTGLDEALNA GAWAVEFDYS GFNAT..... GGGPGSVIPL
DesulfCprA IGAIKAPAKV ANAAETMNYV PGPTNARSKL RPVHDFAGAK VRFVENNDEW
Consensus .....g ....d...ya ....p.....
201 250
VcrA WGLYGPPHDS APPD...GSV PKWEGTPEDN FLMLRAAAKY FGAGGVGALN
DmccaTceA MNGINGLHEF GHADIKTTNY PKWEGTPEEN LLIMRTAARY FGASSVGAIK
DEth195 MNGINGLHEF GHADIKTTNY PKWEGTPEEN LLIMRTAARY FGASSVGAIK
SmultivoPceA WSGETMTNTQ LWAPV...GL DRRPPDTTDP V..... ....ELTNYV
DesulfH YPINPMTNEI ANEPVMVPGL YNWDNIDVES VRQQGQQWKF ESKEEASKIV
DesulfCprA LGTTKIISKV KKTSEADAGF MQAVRGLYGP DPQRGFFQFI AKHPFGGTIS
Consensus ....g. ..w..... ....g.i.
251 300
VcrA LADPKCKKLI YKGAQPMTLG KGTYSEIGGP GMIDAKIYPK VPDHA...VP
DmccarTceA ITD.NVKKIF YTKAQPFSLG PW.YTITNFA EYIEYPV..P VDNYA...IP
DEth195 ITD.NVKKIF YAKVQPFCLG PW.YTITNMA EYIEYPV..P VDNYA...IP
SmultivoPceA KFAARMAGAD LVGVARLN.R NWVYS...EA VTIPADVPYE QSLHKEIEKP
DesulfH KKATRLLGAD LVGIAPYD.E RWTYSTWGRK IYKPCKMPNG RTKYLPWDLP
DesulfCprA WARNLIAAED VVDGDAEPTK TPIPDPEQMS QHIRDCCYFL RADEVGIGKM
Consensus .....d .v...p.... .w.ys..... ..i..... .....p

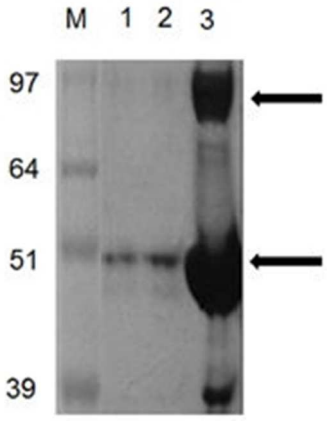
M
1
2
3
97
64
51
39

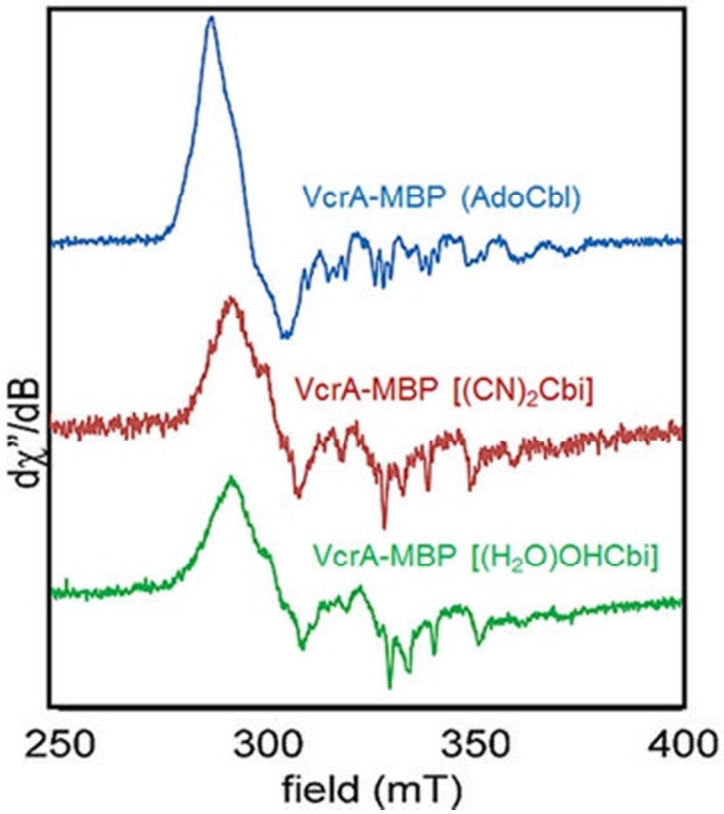
VcrA-MBP (AdoCbl)
VcrA-MBP [(CN)2Cbi]
VcrA-MBP [(H2O)OHCbi]
dχ"/dB
250
300
350
400
field (mT)

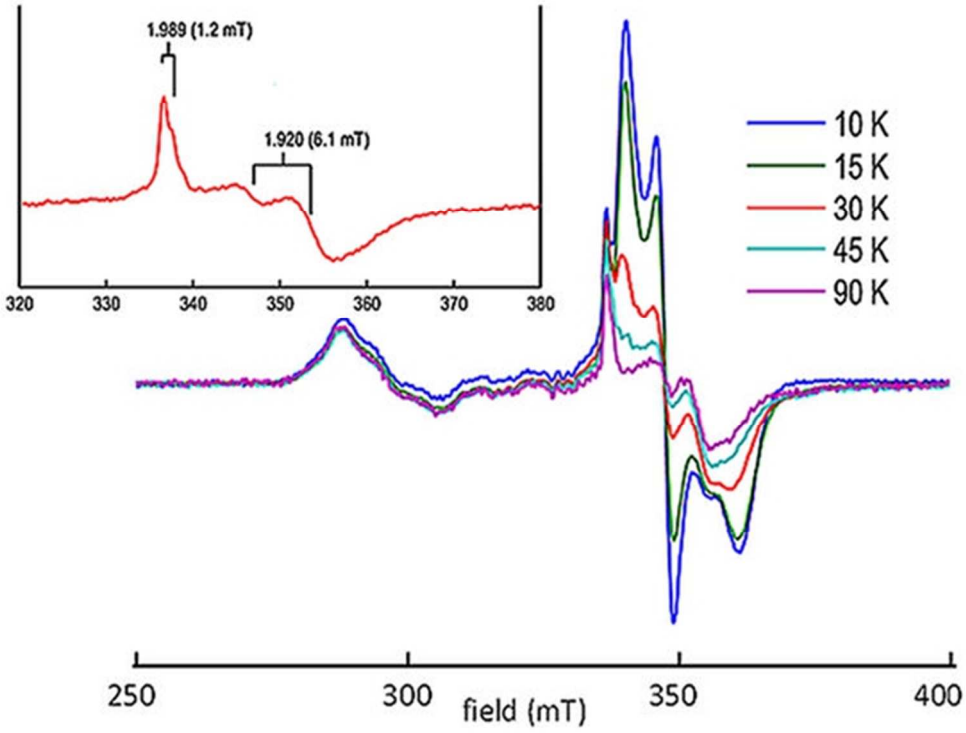
1.989 (1.2 mT)
1.920 (6.1 mT)
320
330
340
350
360
370
380
10 K
15 K
30 K
45 K
90 K
250
300
350
400
field (mT)

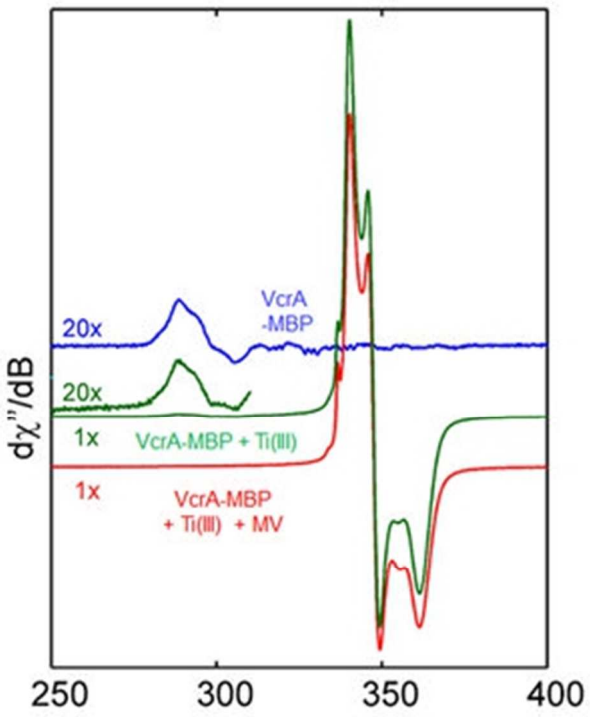
VcrA
-MBP
20x
20x
1x
VcrA-MBP + Ti(III)
1x
VcrA-MBP
+ Ti(III) + MV
dχ''/dB
250
300
350
400

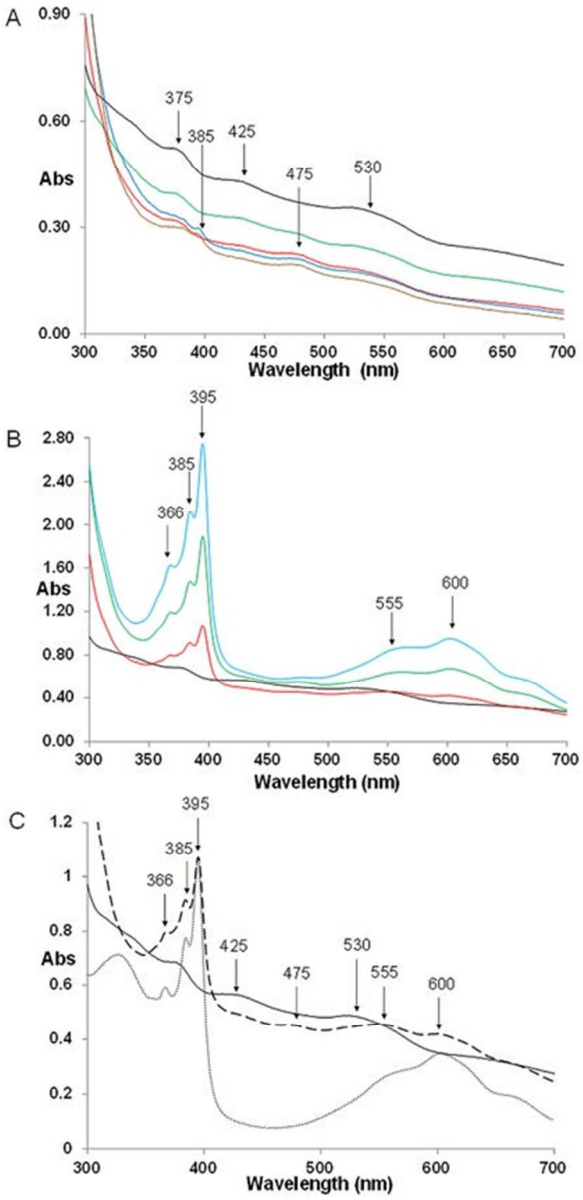
A
0.90
0.60
0.30
0.00
Abs
375
385
425
475
530
300 350 400 450 500 550 600 650 700
Wavelength (nm)
B
2.80
2.40
2.00
1.60
1.20
0.80
0.40
0.00
Abs
395
385
366
555
600
300 350 400 450 500 550 600 650 700
Wavelength (nm)
C
1.2
1
0.8
0.6
0.4
0.2
0
Abs
395
385
366
425
475
530
555
600
300 400 500 600 700
Wavelength (nm)

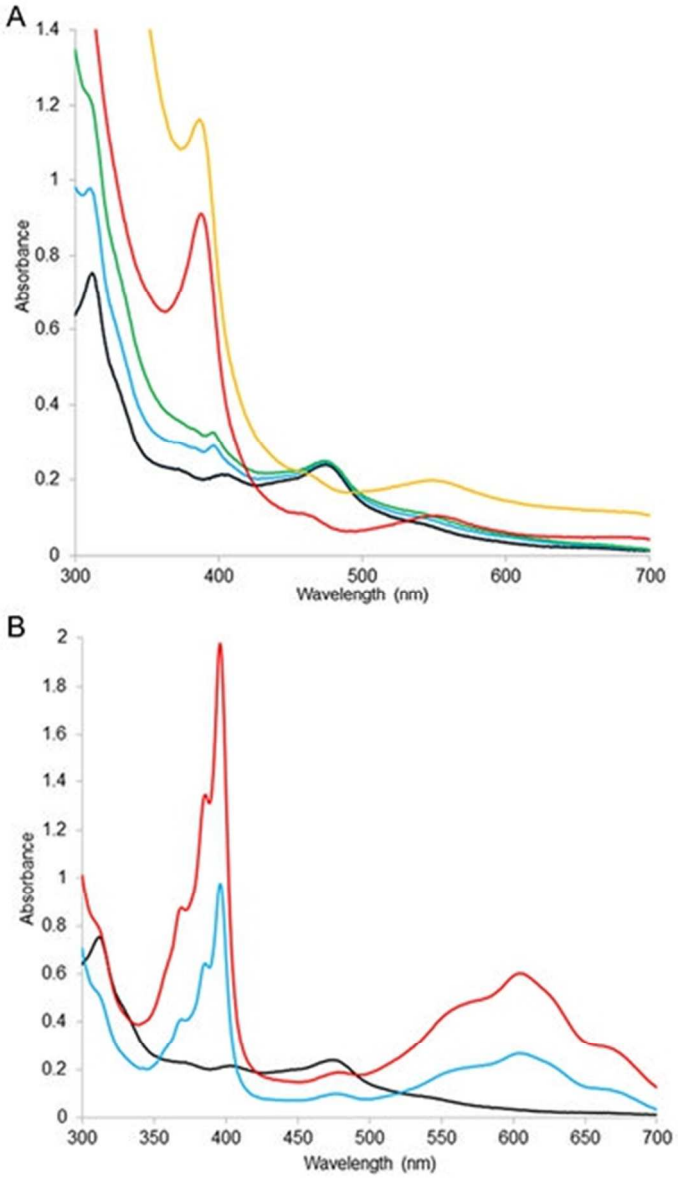
A
Absorbance
Wavelength (nm)
B
Absorbance
Wavelength (nm)

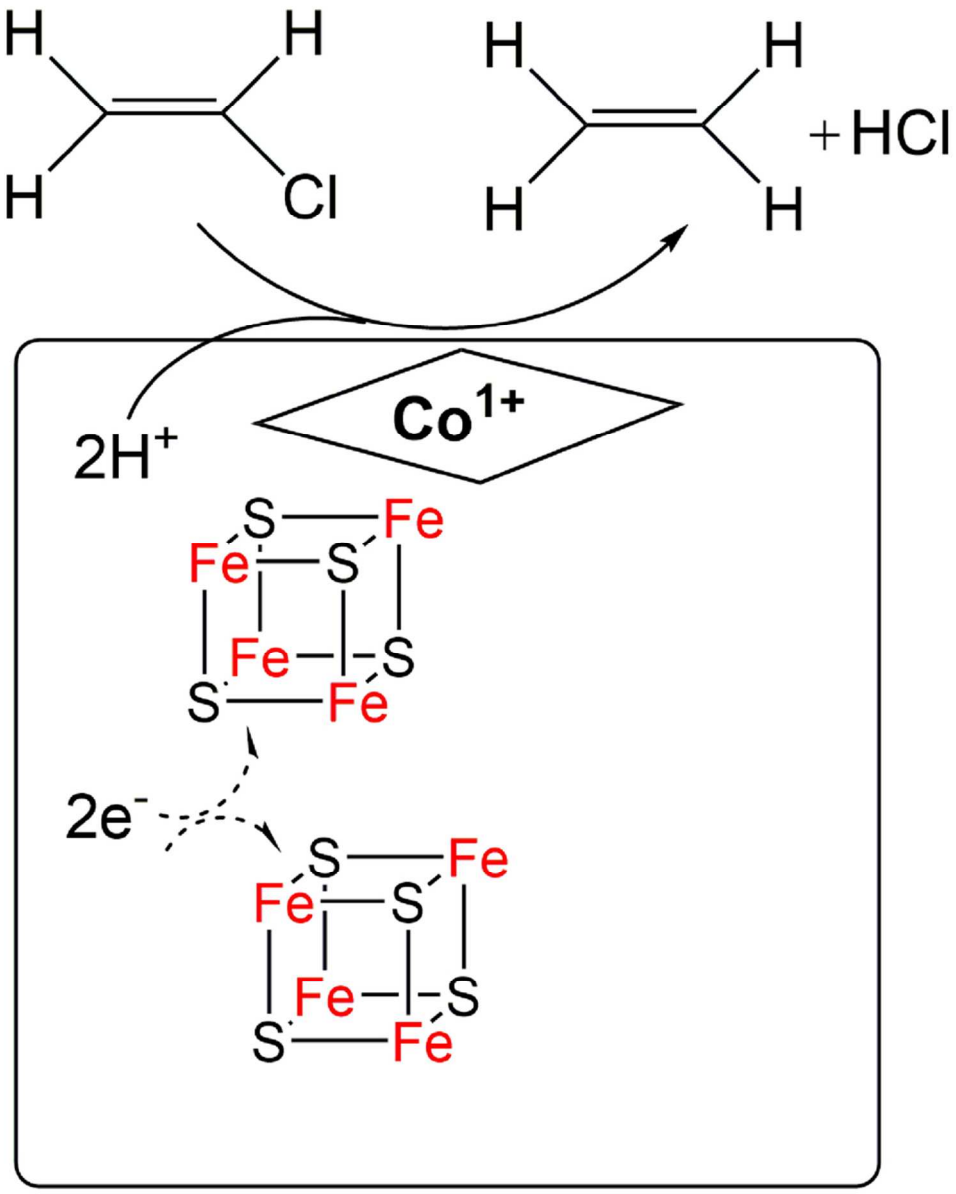

81x100mm (300 x 300 DPI)